Study of I−(CO2) n , Br−(CO2) n , and I−(N2O) n clusters by anion photoelectron spectroscopy

Don W. Arnold, Stephen E. Bradforth, Eun H. Kim, and Daniel M. Neumark

Citation: The Journal of Chemical Physics **102**, 3510 (1995); doi: 10.1063/1.468576
View online: http://dx.doi.org/10.1063/1.468576
View Table of Contents: http://scitation.aip.org/content/aip/journal/jcp/102/9?ver=pdfcov
Published by the AIP Publishing

Study of $I^-(CO_2)_n$, $Br^-(CO_2)_n$, and $I^-(N_2O)_n$ clusters by anion photoelectron spectroscopy

Don W. Arnold,[a] Stephen E. Bradforth,[b] Eun H. Kim, and Daniel M. Neumark[c]
Department of Chemistry, University of California, Berkeley, California 94720
and Chemical Sciences Division, Lawrence Berkeley Laboratory, Berkeley, California 94720

(Received 12 September 1994; accepted 23 November 1994)

Photoelectron spectra of the $I^-(CO_2)_{n=1-13}$, $I^-(N_2O)_{n=1-12}$, and $Br^-(CO_2)_{n=1-11}$ clusters are presented. The spectra provide information about the stepwise solvation of the bromide and iodide anions and about the size of the first solvation shells in these clusters. The data suggest that significantly different solute–solvent interactions exist in the three sets of clusters studied here. The $X^-(CO_2)_n$ spectra exhibit resolved progressions which are assigned to in-phase CO_2 solvent bending vibrations in the neutral clusters. These vibrations are excited by photodetachment of anion clusters in which the CO_2 molecules are distorted from linearity by a charge-quadrupole interaction. The $I^-(N_2O)_n$ spectra do not show any vibrational structure, presumably because the weaker ion–solvent interactions are insufficient to distort the N_2O molecules. © *1995 American Institute of Physics.*

I. INTRODUCTION

The study of molecular clusters has developed into a diverse field directed towards understanding the evolution of molecular interactions from simple gas-phase dimers to bulk chemical material. An important subset of cluster research involves the stepwise solvation of a chromophore, so that one can follow how its properties change as a function of the number and type of solvent molecules. If the chromophore is an ion, the resulting ion clusters can be readily mass selected, which makes them especially amenable to kinetic, thermodynamic, and spectroscopic studies of this type.[1] From cluster ion mass spectroscopy and thermochemistry, one can learn about solvation energetics and infer the existence and size of particularly stable ''solvent shells;'' such experiments have been performed with great success by Kebarle,[2] Castleman,[3] Hiraoka,[4] and Meot-ner.[5]

In recent years, numerous optical spectroscopy experiments have been carried out on cluster ions; these hold the promise of providing more detailed information on cluster structure and dynamics than experiments which rely solely on mass spectroscopy. In studies of positive ion clusters, the vibrational predissociation experiments of Lee,[6] Lisy,[7] Stace,[8] and Okumura[9] and the electronic spectroscopy experiments of Miller[10] and Maier[11] have used the spectral patterns and shifts with cluster size as a detailed probe of cluster structure. Lineberger and co-workers have used photodissociation spectroscopy to study the effects of clustering on both positive and negative ions.[12,13]

However, most spectroscopic studies of negative ion clusters have been performed with photodetachment techniques, namely photoelectron spectroscopy (PES) and zero electron kinetic energy (ZEKE) spectroscopy, both of which combine mass selectivity with reasonable spectral resolution. The negative cluster ions studied by these techniques can, for the most part, be divided into two groups. Several studies have been completed on elemental and molecular clusters of the type A_n^-, in which the negative charge is fairly delocalized; these have been carried out in our laboratory[14] as well as those of Smalley,[15] Lineberger,[16] Meiwes-Broer,[17] Bowen,[18] Johnson,[19] and Eberhardt.[20] The second group of clusters is of the form, $X^-(M)_n$, where the charge remains localized on a single chromophore, X^-, that interacts with solvent molecules, M. The signature of this type of cluster is that the photodetachment spectrum retains the primary features associated with the X^- species because of the relatively weak X–M interactions. Photoelectron spectra of $X^-(M)_n$ clusters have been obtained in several of the laboratories mentioned above,[21,22,23] as well as by the Cheshnovsky[24,25] and Kaya[26] groups. This paper focuses on clusters of the latter type. We are specifically interested in the solvation of I^- and Br^- by CO_2 and N_2O. This work is an extension of the preceding paper[27] which was concerned with the binary $X^-(CO_2)$ complexes, with X═F, Cl, Br, and I.

Related studies of this type have been carried out in other laboratories as well as our own. In the first study of X^-/CO_2 clusters, Markovich *et al.*[24] obtained photoelectron spectra of $I^-(CO_2)_{n=1-7}$ in order to probe the solvation energetics of these clusters. Markovich *et al.*[25] have also used this technique to study hydrated iodide clusters, $I^-(H_2O)_{n\leqslant 60}$. From their results, they suggest the formation of a solvent shell around I^- composed of 6 H_2O molecules. They also assign features in some of their spectra to another isomer of the cluster in which the I^- resides on the surface of a water cluster rather than in the center. In our laboratory,[22] we have reported photoelectron spectra of the clusters $I^-(CO_2)_{n=1-13}$. The higher resolution in these spectra (10 meV) as compared to those of Markovich *et al.*,[24] revealed vibrational structure which indicated that the I^-–CO_2 interaction in the anion clusters was strong enough to bend the CO_2 solvent molecules. The nature of this interaction is discussed in detail in the preceding paper[27] on binary $X^-(CO_2)$ complexes. We have also measured the ZEKE spectrum of $I^-(CO_2)$ at a resolution of 0.3–0.4 meV.[28] This spectrum yielded the splitting of the $I(^2P_{3/2})$ level due to its

[a]Present address: Department of Chemistry, University of Southern California, Los Angeles, California 90025.
[b]Present address: Department of Chemistry, University of Chicago, Chicago, Illinois 60637.
[c]Camille and Henry Dreyfus teacher–scholar.

 0021-9606/95/102(9)/3510/9/$6.00

interaction with the CO_2 in the neutral complex and the frequencies of the low frequency C–I stretching modes in the anion and neutral; from this we obtained detailed I^-/CO_2 and I/CO_2 potentials.

In this study, we present and discuss the photoelectron spectra of $I^-(CO_2)_{n=1-13}$, $Br^-(CO_2)_{n=1-11}$, and $I^-(N_2O)_{n-12}$ in order to study the evolution of the solute–solvent interactions as a function of solute, solvent, and size. The two solvent species, N_2O and CO_2, are isoelectronic and the two chromophores are both halides, I^- and Br^-. Nonetheless, as will be seen, the spectra clearly show that the ion–solvent interactions for all three systems studied are different. While both the $I^-(CO_2)_n$ and the $Br^-(CO_2)_n$ spectra suggest that the similar ion–CO_2 interactions exist in two types of clusters, the stepwise solvation energies indicate that the size of the first solvent shell is smaller for the $Br^-(CO_2)_n$ clusters, and that the solvent–solute binding is considerably stronger in the first solvent shell of $Br^-(CO_2)_n$ clusters. The vibrational structure seen in many of the $I^-(CO_2)_n$ and $Br^-(CO_2)_n$ spectra also point to stronger interactions in the $Br^-(CO_2)_n$ clusters. The $I^-(N_2O)_n$ spectra, which differ significantly from those of the CO_2 clusters, show that the I^-/N_2O interaction is weaker, resulting in no distortion of the N_2O and a larger solvent shell around the I^- chromophore.

II. EXPERIMENT

The apparatus employed in these experiments, a dual time-of-flight anion photoelectron spectrometer, has been described in detail previously.[27,29] An overview of the apparatus, with details relevant to the present results, will be summarized here. Anion clusters are generated at the intersection of a pulsed molecular beam and a 1 keV electron beam.[30] The pulsed molecular beam is made from a gas mixture of 1% HI (or HBr) in a carrier gas (N_2O or CO_2) which is expanded through a piezoelectric valve operated at 20 Hz with a stagnation pressure of ~3–4 atm. I^- and Br^- ions are formed by dissociative attachment of low-energy (~1 eV) secondary electrons to HI and HBr. As the free jet expansion evolves, the ions cluster with the carrier gas and relax rotationally and vibrationally.

The cooled ions are extracted into a Wiley–McLaren-type time-of-flight mass spectrometer[31] where they separate according to mass. The ion of interest is selectively photodetached by a properly timed 8 ns laser pulse. Photoelectron energies are determined by time-of-flight measurements in a 1 m field-free flight tube. The resolution of the apparatus is 0.010 eV for electrons with 0.65 eV of electron kinetic energy (eKE) and degrades as $(eKE)^{3/2}$. For these experiments, the 4th (266 nm; 4.657 eV; 15 mJ/pulse) and 5th (213 nm; 5.822 eV; 6 mJ/pulse) harmonics of a Nd:YAG pulsed laser are employed for photodetachment. The 213 nm photons generate background signal through the interactions of scattered light with the surfaces of the detector chamber. A background spectrum, collected using the same laser power used during data collection, is fitted to a smooth function which is scaled and subtracted from the data to correct for the moderate level background signal.

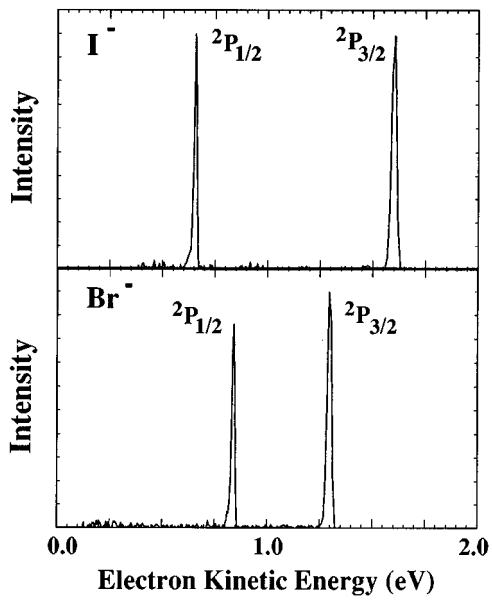

FIG. 1. Photoelectron spectra of I^- and Br^- collected using a photodetachment energy of 4.657 eV.

III. RESULTS

For comparison to the cluster data, photoelectron spectra of I^- and Br^- using a 4.657 eV photodetachment energy are shown in Fig. 1. The spectra represent electron signal as a function of electron kinetic energy (eKE) where

$$\mathrm{eKE} = h\nu - \mathrm{EA} - T_0 - E_v^0 + E_v^- . \tag{1}$$

In Eq. (1), $h\nu$ is the laser photon energy, EA is the electron affinity of the neutral cluster, and T_0 is the term value of the neutral electronic state. In the case of the polyatomic spectra presented below, E_v^0 and E_v^- are the vibrational energies (above the zero point) of the neutral and anion, respectively. The two peaks in each halide spectrum (Fig. 1) represent photodetachment transitions from the closed-shell halide anions to the two spin–orbit states of the halogen atoms. The peaks at high and low eKE in each spectrum represent photodetachment transitions to the halogen ground ($^2P_{3/2}$) and excited ($^2P_{1/2}$) spin–orbit states, respectively. The $^2P_{3/2}$ peaks are slightly broader because they occur at higher eKE. The electron affinities and spin–orbit splitting for each of these atoms are well-known and are listed in the preceding paper.[27]

Shown in Fig. 2 are the photoelectron spectra collected for the $I^-(N_2O)_n$ clusters, $n=1$–12, at a photodetachment energy of 4.657 eV. For $n=1$–3, the spectra contain two peaks separated by an energy equal to that of the iodine spin–orbit splitting. We refer to these peaks as the $I(^2P_{3/2})\cdot(N_2O)_n$ and $I(^2P_{1/2})\cdot(N_2O)_n$ bands; similar notation will be used for the CO_2 clusters discussed below. In Fig. 2, the most obvious change which occurs as a function of cluster size is the consistent shift of the spectra to lower eKE. For the $I^-(N_2O)_3$ cluster, the $^2P_{1/2}$ band state intensity is affected by the cutoff of the experimental detection efficiency. For the larger clusters, the excited state is energeti-

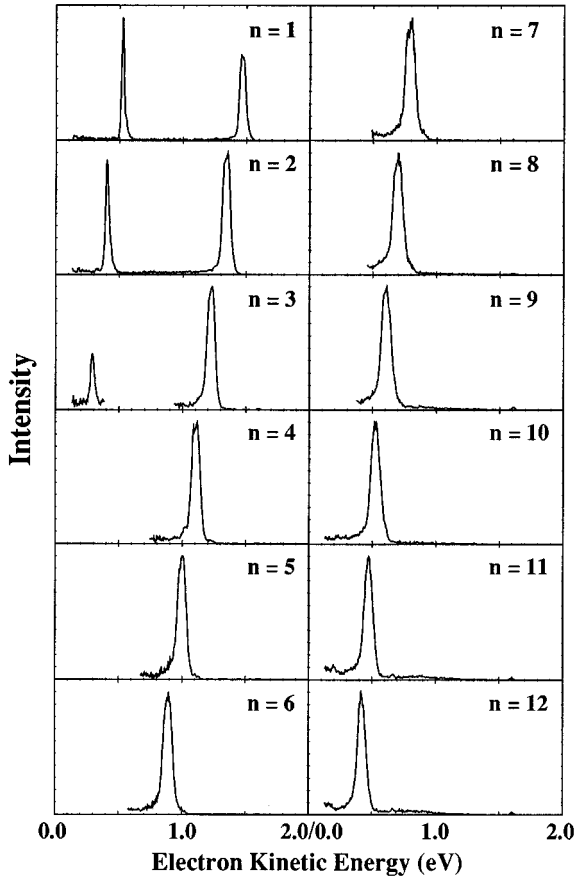

FIG. 2. Photoelectron spectra of $I^-(N_2O)_n$, $n=1$–12, collected using a photodetachment energy of 4.657 eV.

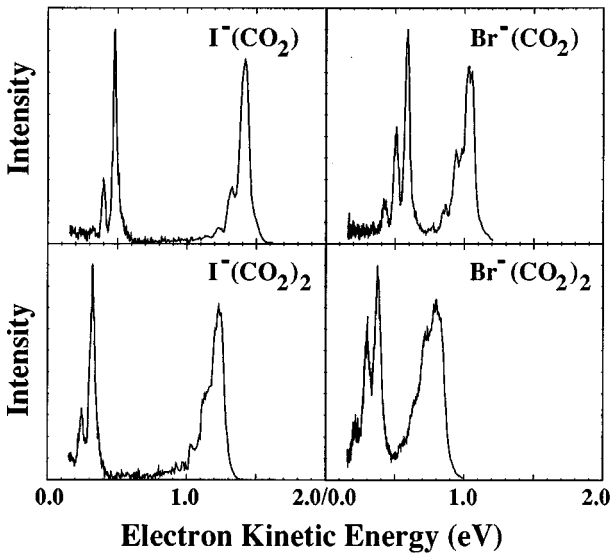

FIG. 3. Photoelectron spectra of $I^-(CO_2)_n$ and $Br^-(CO_2)_n$, $n=1$–2, using a photodetachment energy of 4.657 eV.

cally out of range at the photodetachment energy used. The peaks at high eKE are significantly broader than the peaks at low eKE. The peak widths are larger than would be expected by the experimental resolution function for individual transitions, suggesting the presence of underlying structure.

Figure 3 displays the photoelectron spectra of $I^-(CO_2)_n$ and $Br^-(CO_2)_n$, $n=1,2$ collected at photodetachment energy of 4.657 eV. As in the $I^-(N_2O)_n$ spectra (Fig. 2), the peaks shift to lower energy with increasing cluster size and the general spin–orbit splitting of the halogen atom is preserved. However, the $X^-(CO_2)_n$ spectra show additional structure for each electronic state which extends to low eKE. As discussed previously,[22,27] the additional peaks in the spectrum result from excitation of the CO_2 bending vibration upon photodetachment. The length of the vibrational progression increases as a function of cluster size. The peaks at high eKE are significantly broader than the peaks at low eKE. In the $Br^-(CO_2)$ spectrum, an additional splitting of the peaks in the $^2P_{3/2}$ band is discernible.

Figures 4 and 5 show the photoelectron spectra of $I^-(CO_2)_n$, for $n=0$–13, and $Br^-(CO_2)_n$, for $n=0$–11, respectively, at a photodetachment energy of 5.822 eV. In both sets of data, the vibrational progression in the $^2P_{1/2}$ band becomes more extended as n is increased through $n=5$. In the $Br^-(CO_2)_n$ spectra, no vibrational structure is evident from $n=6$–8, but for $n=9$–11, some structure can be seen in

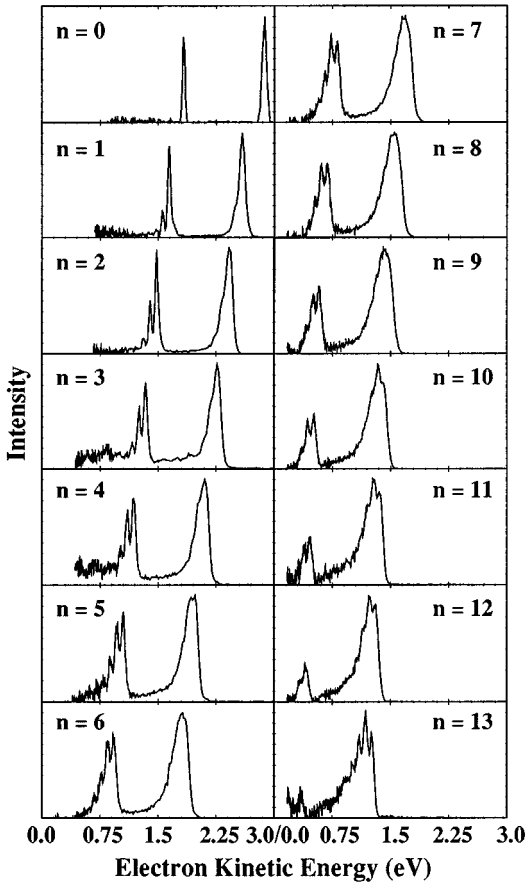

FIG. 4. Photoelectron spectra of $I^-(CO_2)_n$, $n=0$–13, collected using a photodetachment energy of 5.822 eV.

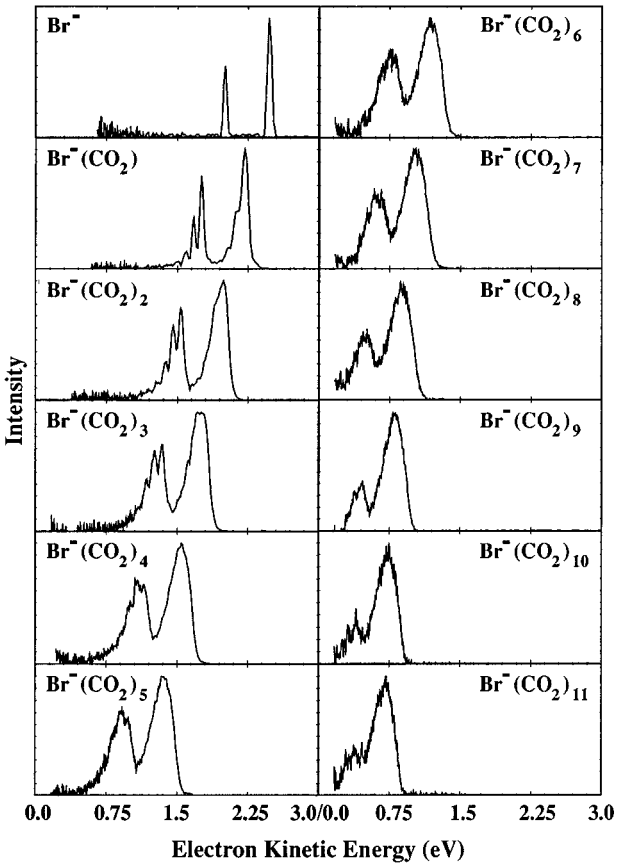

FIG. 5. Photoelectron spectra of $Br^-(CO_2)_n$, $n=0$–11, collected using a photodetachment energy of 5.822 eV.

the $^2P_{1/2}$ band. In contrast, one observes vibrational structure in the $^2P_{1/2}$ band of all the $I^-(CO_2)_n$ spectra until the intensity of the this band is degraded by the detector cutoff function and becomes inaccessible at the 5.822 eV photon energy (i.e., $n>11$). A notable feature of this data set is the *reappearance* of vibrational structure in the $^2P_{3/2}$ band as the size increases past $n=9$, culminating in a distinct progression for the largest cluster studied, $I^-(CO_2)_{13}$. No such reappearance of vibrational structure occurs in the $Br^-(CO_2)_n$ data set.

IV. ANALYSIS AND DISCUSSION

In the following sections, we will treat the data in more detail. The size-dependent solvation thermodynamics are analyzed in Sec. IV A. As part of the interpretation of the thermodynamic information, the dominant bonding interactions and the geometries of the complexes are considered. In Sec. IV B, the vibrational structure observed in the $X^-(CO_2)_n$ photoelectron spectra are discussed in terms of the cluster size and symmetry.

A. Thermodynamics and geometries

As illustrated in Fig. 6, the shift of the photoelectron spectra to lower eKE as a function of cluster size results from the different interactions of the solvent molecule with the anion and neutral. Assuming the 0–0 transition can be identified in the photoelectron spectrum, Eq. (2) shows the

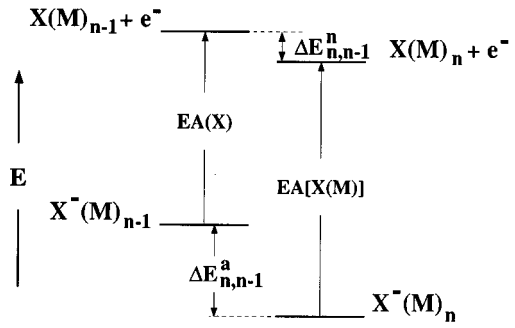

FIG. 6. Schematic diagram of the thermodynamics of solvation for a single solvent molecule. The difference between $\Delta E^a_{n,n-1}$ and $\Delta E^n_{n,n-1}$ leads to the observed spectral shift upon solvation.

relationship between the adiabatic EAs of the two clusters and the charge stabilization provided by a solvent molecule, $\Delta E_{n,n-1}$,

$$\mathrm{EA}_n = \mathrm{EA}_{n-1} + \Delta E^a_{n,n-1} - \Delta E^n_{n,n-1}. \tag{2}$$

$\Delta E^a_{n,n-1}$ and $\Delta E^n_{n,n-1}$ are the stepwise solvation energies (SSE) for the anion and neutral, respectively. The electrostatic forces responsible for most of the binding energy in the anion cluster are considerably stronger than the van der Waals forces in the neutral cluster,[28] so we expect $\Delta E^a_{n,n-1} \gg \Delta E^n_{n,n-1}$. This means that the EA increases with cluster size, and that the anion SSE is given, to a good approximation, by $\Delta E^a_{n,n-1} = \mathrm{EA}_n - \mathrm{EA}_{n-1}$. The electron affinity changes therefore map out how much a given anion cluster is stabilized by the addition of a solvent molecule.

Figure 7 shows the plot of SSE vs cluster size for the three systems. Two sources of peak broadening contribute the uncertainty in the determination of the adiabatic EA's. The peaks are broadened due to unresolved underlying structure which results primarily from excitation of van der Waals progressions upon photodetachment. The second source of broadening, which affects only the $^2P_{3/2}$ bands, results from a splitting of the halogen $^2P_{3/2}$ ground state degeneracy by the solvent molecules.[28] For consistency, the measurement of the EAs (used to determine the SSEs) are made at 25% of the

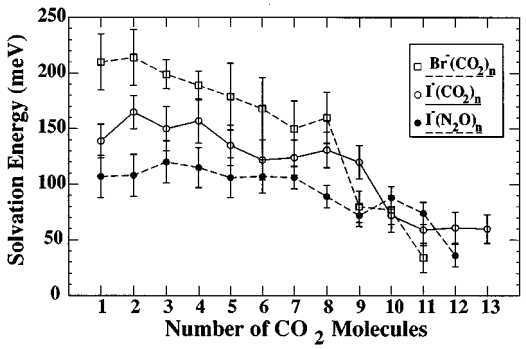

FIG. 7. Plot of the stepwise solvation energy for the $I^-(N_2O)_n$, $I^-(CO_2)_n$, and $Br^-(CO_2)_n$ clusters as a function of the number of solvent molecules. Energies are determined at 25% of the full peak height for the highest eKE feature in each spectrum.

TABLE I. Spectral shifts as a function of stepwise solvation.

	$I^-(N_2O)_n$		$I^-(CO_2)_n$		$Br^-(CO_2)_n$	
n	eKE (eV)	ΔE (meV)	eKE (eV)	ΔE (meV)	eKE (eV)	ΔE (meV)
0	1.600	0	2.77	0	2.460	0
1	1.485	115	2.598	172	2.230	230
2	1.358	127	2.442	156	2.011	219
3	1.242	116	2.283	159	1.792	219
4	1.122	120	2.127	156	1.568	224
5	1.006	116	1.993	134	1.387	181
6	0.905	101	1.864	129	1.214	173
7	0.808	97	1.720	144	1.056	158
8	0.715	93	1.587	133	0.897	159
9	0.612	103	1.467	120	0.820	77
10	0.535	77	1.430	37	0.741	79
11	0.492	43	1.385	45	0.720	21
12	0.434	58	1.316	70	⋯	⋯
13	⋯	⋯	1.270	46	⋯	⋯

full height of the peak at highest eKE for each cluster. The peak position and SSE's are summarized in Table I.

The data show that for the first several solvent molecules, the ordering of the SSE's is $Br^-(CO_2)_n > I^-(CO_2)_n > I^-(N_2O)_n$. The first several CO_2 and N_2O molecules added to the cluster provide approximately equal stabilization of the halide charge. This behavior is in agreement with a previous study of $I^-(CO_2)_{n=1-7}$, where Markovich *et al.* also observe approximately equal SSEs for these clusters.[24] However, above a certain cluster size, the SSE decreases abruptly for all three series. The dropoffs occur after $Br^-(CO_2)_{n=8}$, $I^-(CO_2)_{n=9}$, and $I^-(N_2O)_{n=11}$. It is apparent that the additional solvent molecules bind to the clusters through different, weaker interactions. This implies that that these three cluster sizes represent the formation of the first solvent shell around the halide anion, resulting in a significant shielding of the charge from any additional solvent molecules. The larger shell size indicated for $I^-(N_2O)_n$ vs $I^-(CO_2)_n$ is consistent with the stronger interaction between I^- and CO_2 as evidenced from the SSE's; one expects the N_2O molecules to form a ''looser'' shell about the I^-, so it is not surprising that the size of this shell is larger. The smaller shell size implied for the $Br^-(CO_2)_n$ clusters is also expected, given that Br^- is smaller than I^- and that the Br^- interaction with CO_2 is stronger than the I^-/CO_2 interaction.

A similar analysis by Markovich *et al.*[25] indicates that the first solvent shell for $I^-(H_2O)_n$ clusters occurs at $n=6$. The smaller H_2O solvation shell, as compared to CO_2, is consistent with the stronger binding with H_2O; the well depth for $I^-(CO_2)$ is 0.212 eV,[28] whereas ΔH for $I^-(H_2O)$ dissociation is 0.44 eV.[32] The stronger interactions will results in shorter halide–solvent separations which, in turn, will result in a smaller solvation shell due to steric effects. There has been some controversy regarding the interpretation of the $I^-(H_2O)_n$ PES data; calculations by Berkowitz[33] and Garrett[34] have suggested that halide anions reside on the surface of the water clusters, while recent calculations by Combariza *et al.*[35] support the interpretation of the PES data in terms of a caged iodide anion. The surface structure is favorable in the $I^-(H_2O)_n$ clusters as it allows for maximum hydrogen bonding among the H_2O molecules. The attractions between CO_2 molecules are weaker, however; $D_e \cong 0.10$ eV for $(CO_2)_2$.[36] It is therefore reasonable to expect maximum solvation of the I^- in the lowest energy $I^-(CO_2)_n$ structure.

Our results can also be compared with the photodissociation experiments by Lineberger and co-workers[13] on $Br_2^-(CO_2)_n$ and $I_2^-(CO_2)_n$ clusters. They found that $n=14$ and $n=16$ are the minimum number of solvent molecules required form complete caging of the Br_2^- and I_2^-, respectively, and interpret these values of n to be the size of the first solvent shell for these clusters. This interpretation is supported by the simulations of Amar and Perara.[37] One expects the size of the first solvent shells for $Br^-(CO_2)_n$ and $I^-(CO_2)_n$ clusters to be somewhat larger than half of those for $Br_2^-(CO_2)_n$ and $I_2^-(CO_2)_n$ clusters, and that is indeed what is implied by the SSE's in Fig. 7. Finally, Bowen and co-workers[38] have recently measured photoelectron spectra of $O^-(Ar_n)$ clusters and find strong evidence for a shell closing at $n=12$ based on their measured SSE's.

A more detailed examination of the SSE's in Fig. 7 shows that as the first solvation shell is being filled, the SSE's for the I^-/CO_2 and I^-/N_2O clusters remain relatively constant, on the average, while those for the Br^-/CO_2 clusters appear to decrease systematically. This suggests that in the I^- based clusters, the nature of the binding sites for the solvent molecules in the first shell does not vary much with the size of the cluster, but this may not be the case in the Br^- clusters. This point is considered further when the vibrational structure in the spectra is discussed below.

The results presented in Fig. 7 show that the SSE's for the $I^-(N_2O)_n$ clusters are consistently lower than those for $I^-(CO_2)_n$ and $Br^-(CO_2)_n$ clusters. This is rather surprising in light of the fact that the charge-dipole is a stronger interaction than the charge-quadrupole interaction which is expected to be the dominant term in the $X^-(CO_2)_n$ clusters. There are several effects which may contribute to this result. Since these clusters are weakly bound, the thermodynamics and geometries are determined primarily by the dominant electrostatic interactions involved. By considering the $X^-(CO_2)$ and $X^-(N_2O)$ long-range electrostatic interactions

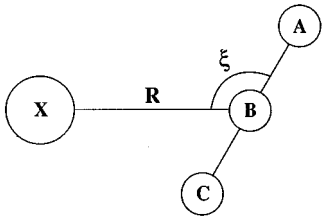

FIG. 8. Schematic diagram of $X^-(M)_n$ complex with coordinates used in the electrostatic calculations. In the figure, X=I or Br and $A-B-C$=O–C–O or N–N–O, in order. Note that for N_2O the variable, R, refers to the distance from the halide to the center of charge of the molecule, which is not the same as the center of mass.

using the known properties of the CO_2 and N_2O molecules, a qualitative understanding of the observed results is obtained.

While CO_2 and N_2O are isoelectronic molecules, they possess slightly different electrostatic properties, leading to a significantly different interaction with the halides. As discussed in detail previously,[27] the leading term in the X^-–CO_2 interaction is the charge-quadrupole interaction,

$$E_{q\Theta}=\frac{q\cdot\Theta}{2R^3}\,[3\cdot\cos^2(\xi)-1], \tag{3}$$

where $q=-e$ is the halide charge and Θ is the quadrupole of the CO_2 molecule [$\Theta_{CO_2}=-(4.3\pm0.14)\times10^{-26}$ esu cm^2].[39] The geometrical variables, R and ξ, are illustrated in Fig. 8. The negative sign of Θ indicates that the carbon atom is positively charged relative to the oxygen atoms. According to Eq. (3), the $X^-(CO_2)$ cluster will be T-shaped. However, as shown previously,[27] the charge-quadrupole interaction actually distorts the CO_2 molecule from linearity. The CO_2 distortions were determined by a Franck–Condon analysis of the photoelectron spectra to be $\theta_{OCO}=174.5\pm1.5°$ for $I^-(CO_2)$ and $172.2\pm1.5°$ for $Br^-(CO_2)$. This distortion presumably causes the vibrational structure seen in the photoelectron spectra of the larger clusters containing CO_2 as well.

In contrast, no vibrational structure is observed in the $I^-(N_2O)_n$ spectra. This implies that the N_2O solvent molecules are not significantly distorted by the core ion. To understand the different binding for the $I^-(N_2O)$ clusters, one must consider the both charge-dipole and charge-quadrupole interactions because N_2O has a small dipole moment ($\mu_{N_2O}=0.1608$ D; $\overset{+}{N}-N-\overset{-}{O}$) (Ref. 40) and a quadrupole moment [$\Theta_{N_2O}=-(3.36\pm0.18)\times10^{-26}$ esu cm^2] (Ref. 41) which is slightly less than that of the CO_2 molecule. The charge-dipole energy expression is given in Eq. (4),

$$E_{q\mu}=\frac{q\cdot\mu\cdot\cos(\xi)}{R^2}, \tag{4}$$

where μ is the N_2O dipole. This favors a linear X^-–N–N–O orientation in contrast to the charge-quadrupole interaction.

Although one normally expects electrostatic interactions involving lower order moments to dominate, the dipole and quadrupole moments of N_2O are such that the charge-quadrupole interaction is considerably stronger over the range of internuclear distances expected for these species. Our ZEKE study[28] of $I^-(CO_2)$ yielded $R_{C-I}=3.8$ Å, so a separation of 4 Å between the charged and neutral particles is a reasonable upper bound to expect for $I^-(N_2O)$. At this distance, as ξ varies from 0 to $\pi/2$, $E_{q\mu}$ increases from -0.03 eV to 0 while $E_{q\Theta}$ drops from 0.157 eV to -0.079 eV. The energy minimum in the sum of the two terms is very close to $\xi=\pi/2$, so we expect that $I^-(N_2O)$ is nearly T-shaped. Thus, $E_{q\mu}$ appears to act only as a slight perturbation, and will become even less important at smaller values of R_{C-I}. The lack of distortion of the N_2O moiety may be due simply to the smaller quadrupole moment of N_2O compared to CO_2; the electrostatic interaction responsible for the distortion may not be strong enough to compensate for the concomitant strain energy associated with bending the N_2O [Eq. (8) of preceding paper[27]].

B. Vibrational structure

As we have discussed previously,[22,27] the relaxation of the CO_2 solvent molecules from a bent to linear geometry upon photodetachment of the $X^-(CO_2)_n$ species results in the vibrational progressions seen in the photoelectron spectra. The lengthening of this vibrational progression as the cluster increases in size is quite interesting and provides information about the stepwise solvation of the halide anion. In general, the longer progression suggests a larger displacement along the relevant normal coordinate of vibration in the cluster. While a zero-order interpretation of this result suggests that the CO_2 subunits become more distorted as the cluster size increases, a more detailed analysis of the vibrations reveals that, in fact, the individual CO_2 molecules are distorted by an approximately equal or lesser amount as the cluster grows.

We consider the photodetachment of an $X^-(CO_2)_n$ cluster in which all OCO angles and bond strengths (i.e., force constants) are the same as that of the binary complex, $X^-(CO_2)$. Photodetachment should primarily excite the collective CO_2 bending vibration in which all of the CO_2 molecules vibrate in-phase with each other. The extent of the observed vibrational progression in the photoelectron spectrum is determined by $\Delta Q_n^{CO_2}$, the displacement along the normal coordinate for this in-phase bend between the anion and the neutral clusters. Assuming the change in θ_{OCO} upon photodetachment for each CO_2 molecule is independent of cluster size, the appropriate normal coordinate for the collective in-phase bend can be derived by treating the n vibrating CO_2 molecules as an ensemble of equivalent, uncoupled, one-dimensional harmonic oscillators. Suppose $Q_1^{CO_2}$ is the value of the CO_2 bend normal coordinate of the $I^-(CO_2)_{n=1}$ cluster. For a cluster containing n CO_2 molecules, each with θ_{OCO} equal to that found in the binary complex, the properly normalized normal coordinate[42] is given by $Q_n^{CO_2}=\sqrt{n}\cdot Q_1^{CO_2}$. This means that if the clusters $I^-(CO_2)$ and $I^-(CO_2)_n$ are photodetached, and identical changes occur in all of the OCO angles, the normal coordinate displacement for the larger cluster, $\Delta Q_n^{CO_2}$, is enhanced relative to $\Delta Q_1^{CO_2}$ by

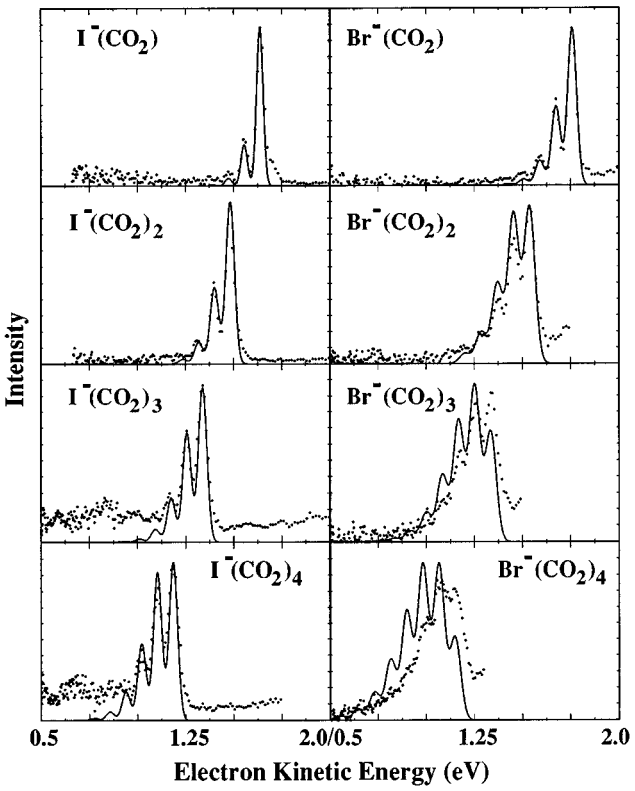

FIG. 9. Comparison of Franck–Condon simulations performed under the constraints of Eq. (5) with the photoelectron spectra of $I^-(CO_2)_n$ and $Br^-(CO_2)_n$, $n=1-4$. See text for details.

$$\Delta Q_n^{CO_2} \approx \sqrt{n} \cdot \Delta Q_1^{CO_2}. \tag{5}$$

Therefore, if θ_{OCO} is independent of n in the anion clusters and equal to 180° in all of the neutral clusters, then Eq. (5) predicts longer vibrational progressions as n increases.

Shown in Fig. 9 are comparisons of Franck–Condon simulations performed under the constraint of Eq. (5) with the $I^-(CO_2)_{n=1-4}$ and $Br^-(CO_2)_{n=1-4}$ experimental data. The simulations are compared with the $^2P_{1/2}$ region of the spectrum; the $^2P_{3/2}$ data are complicated by transitions to the two subcomponents of the $^2P_{3/2}$ state which are split by the solvent molecules.[28] The lengths of the CO_2 bending progressions are the same for the ground and excited state bands since they are primarily determined by the CO_2 distortion in the anion cluster. In the photoelectron spectra, the intensities of the vibrational peaks, I, are determined by the Franck–Condon factors (FCFs) as in Eq. (6),

$$I = v_e \cdot |\tau_e|^2 \cdot |\langle \psi_{v'}(Q'_{CO_2}) | \psi_{v''}(Q''_{CO_2}) \rangle|^2. \tag{6}$$

In Eq. (6) τ_e is the electronic transition dipole, which is assumed to be constant over the energy range of the vibrational progression and v_e is the asymptotic velocity of the photoelectron.[43] As in the previous paper, harmonic oscillator wave functions are used for the CO_2 bend. The normal coordinate displacements $\Delta Q_1^{CO_2}$ for the $I^-(CO_2)$ and $Br^-(CO_2)$ photodetachment are determined by fitting the vibrational progressions,[27] and for the higher clusters, the displacements are given by Eq. (5). The FCFs are convoluted with the experimental resolution function plus an additional Gaussian with a full-width at half-maximum (FWHM) of ~15 meV (to account for unresolved van der Waals progressions) for comparison to the experimental data.

The agreement between data and simulations for $I^-(CO_2)_n$ is excellent for the four spectra shown suggesting that the above structural considerations are indeed plausible. The agreement of the $I^-(CO_2)_n$ simulations with the data strongly suggest that the CO_2 molecules surround the iodide anion in equivalent positions (at least through $n=4$). This is consistent with the results of a distributed multipole analysis presented in the previous paper, illustrating that the solvent CO_2 distortion is well modeled by considering only electrostatic interactions. Thus, if there is negligible interaction among the CO_2 solvent molecules, each will have an identical interaction with the halide. As a result, all of the CO_2 molecules are equally distorted.

However, the agreement for the $Br^-(CO_2)_n$ data are not as good. The simulations overestimate the vibrational excitation for the larger clusters, implying that the OCO angles in $Br^-(CO_2)_n$ become more linear, on average, as a function of cluster size. This suggests that different clustering interactions are involved for $I^-(CO_2)_n$ vs $Br^-(CO_2)_n$. As discussed in the previous paper, charge transfer is expected to contribute more to the distortion of CO_2 in $Br^-(CO_2)$ than in $I^-(CO)_2$. If this is so, then the addition of another CO_2 to $Br^-(CO_2)$ might result in a both solvent molecules becoming more linear because the degree of charge transfer per solvent molecule decreases. This would also lead one to expect a slight decrease in the SSE's with increasing n for the $Br^-(CO_2)_n$ series. As discussed above, this trend is indeed observed in the SSE's plotted in Fig. 7.

An interesting trend in the $^2P_{1/2}$ band of the $Br^-(CO_2)_n$ spectra is the gradual disappearance of vibrational structure as n increases from 4–8 and its re-emergence for $n>8$. The model used for simulating the $n=1-4$ spectra does not predict such an effect, since only one mode of the cluster is assumed to be active and its frequency does not change with cluster size. In reality, however, the low frequency modes of the cluster involving overall motion of the solvent molecules are expected to be active in the photoelectron spectrum, so that each feature in the photoelectron spectrum actually represents the envelope of one or more unresolved progressions. This was explicitly seen in the $I^-(CO_2)$ ZEKE spectrum, which showed extensive progressions in the low frequency C–I stretch (64 cm^{-1} in the anion and 30 cm^{-1} in the neutral).[28] If these progressions become more extended for larger cluster sizes, the features in the photoelectron spectrum associated with the high frequency CO_2 bend will broaden and overlap to the point where they cannot be resolved.

More extended progressions in the solvent modes might occur in the larger clusters simply because of larger normal coordinate displacements between the anion and neutral cluster minimum energy configurations. This would broaden the features in the photoelectron spectrum even if all the cluster anions were in their ground vibrational state. Alternatively, this effect could arise from differences in cluster temperature as a function of size. For example, if the $n=8$ clusters are

warmer than the $n=3$ clusters, more anion solvent modes will be excited, and the features in the photoelectron spectrum would clearly be broader for the warmer clusters.

Bowen and co-workers[38] interpreted a variation in the observed peak widths of $O^-(Ar_n)$ cluster photoelectron spectra using such a temperature argument. For the $n=12$ cluster, a maximum in the SSE indicated a closing of the first solvent shell and the peaks were noticeably broader than those of the nearby clusters. They argued that since smaller clusters are formed from larger ones by evaporative cooling,[7,44] then the $n=12$ clusters should be warmer than the nearby clusters because the solvent molecules are more strongly bound in the $n=12$ cluster and are less likely to evaporate for a given cluster temperature. Such an argument is consistent with the reappearance of vibrational structure in the $Br^-(CO_2)_n$ spectra for $n>8$; the $n=8$ cluster represents the formation of a solvent shell, and the SSE drops substantially for $n>8$, so that the larger clusters should be colder than those for which $n\leqslant 8$. For the $I^-(CO_2)_n$ clusters, Fig. 7 shows that the SSE's are smaller for the first solvent shell and the drop in the SSE is smaller for $n>9$. Thus, one might expect lower temperatures overall for the $I^-(CO_2)_n$ clusters, as well as less variation with cluster size. This is consistent with the observation of vibrational structure in the $^2P_{1/2}$ band of all the $I^-(CO_2)_n$ spectra.

While temperature effects may account for differences in the vibrational structure between the $^2P_{1/2}$ bands of the $Br^-(CO_2)_n$ and $I^-(CO_2)_n$ spectra, they cannot explain the differences between the $^2P_{3/2}$ and $^2P_{1/2}$ bands of the $I^-(CO_2)_n$ spectra since these originate from the same anion populations. The $^2P_{3/2}$ vibrational progression is only partially resolved at $n=2$ in the 4.657 eV data (Fig. 3). No resolved features are observed for the $^2P_{3/2}$ band in the 5.822 eV data until the cluster size reaches $I^-(CO_2)_{n=10}$. At this point, a vibrational progression not only *reappears* but also *becomes better resolved* as additional CO_2 molecules are added. While the resolution of the apparatus does improve at lower eKE, this is not sufficient to explain the absence of resolved peaks in the $n=9$ spectrum and their re-emergence in the $n\geqslant 10$ spectra. Of these larger clusters, the most resolved progression is observed in the $I^-(CO_2)_{13}$ spectrum.

This disappearance and reappearance of the vibrational peaks most likely results from the effects of stepwise solvation on the electronic structure of the neutral halogen atom. The approach of the CO_2 molecule to the halogen splits the degeneracy of the halogen $^2P_{3/2}$ ground state. This effectively broadens the peaks in the $^2P_{3/2}$ band and makes the vibrational structure more difficult to resolve. The environment about the I atom may become even more anisotropic with the addition of the next few solvent molecules, resulting in an even larger electronic splitting. However, as the cluster grows large enough for the halogen to be completely surrounded by solvent molecules, the isotropic spatial symmetry of the isolated halogen atom should return. Under such circumstances, the subcomponents of the $^2P_{3/2}$ state become nearly degenerate again and the peaks would narrow, allowing resolution of the vibrational progression. This may be what is happening in the $I^-(CO_2)_n$ spectra. It is interesting to note that the size at which the vibrational structure becomes most prominent ($n=13$) is well beyond the solvent shell size indicated by the SSE data ($n=9$). Further studies on larger clusters may resolve this discrepancy.

In contrast to the $I^-(CO_2)_n$ spectra, the $Br^-(CO_2)_n$ spectra show no evidence for the reappearance of vibrational structure in the $^2P_{3/2}$ band. The spin–orbit splitting in Br is considerably smaller than in I (0.457 eV vs 0.943 eV), and this makes it easier to split the $^2P_{3/2}$ degeneracy in Br. For example, this splitting is 220 cm^{-1} in $I\cdot CO_2$ and 280 cm^{-1} in $Br\cdot CO_2$.[27,28] Moreover, both the SSE's in Fig. 7 and the simulations in Fig. 9 suggest that the addition of CO_2 solvent molecules to the first solvent shell becomes less favorable as the size of the cluster increases, raising the possibility that the CO_2 molecules bound to the Br^- are not equivalent. For the range of cluster sizes studied here, the result of the combining these two effects may be that the environment of the Br atom is never sufficiently symmetric to reduce the $^2P_{3/2}$ splitting to the point where vibrational structure appears in the $^2P_{3/2}$ band. It would clearly be of interest to extend the studies here to larger $Br^-(CO_2)_n$ clusters to see if this structure eventually does reappear, and also to track the $^2P_{3/2}$ splitting as a function of size in simpler clusters such as $Br^-(Ar)_n$. Apkarian[45] has recently presented a treatment of the effect of clustering on the energy levels of a halogen atom, and it will clearly be of interest to apply this to the systems studied here.

V. CONCLUSIONS

Negative ion photoelectron spectroscopy of the $I^-(CO_2)_{n=1-13}$, $I^-(N_2O)_{n=1-12}$, and $Br^-(CO_2)_{n=1-12}$ clusters has been used to investigate and compare the solvation of I^- by CO_2 and N_2O and Br^- by CO_2. The stepwise solvation energies (SSE's) obtained from the photoelectron spectra provide information about the size of the first solvation shell which forms around the halide in the $X^-(CO_2)_n$ and $I^-(N_2O)_n$ clusters. The sudden decrease in the SSE after $I^-(N_2O)_{n=11}$, $I^-(CO_2)_{n=9}$, and $Br^-(CO_2)_{n=8}$ suggests that the first solvation shells for the $I^-(CO_2)_n$ and $I^-(N_2O)_n$ cluster contain nine and eleven molecules while eight CO_2 molecules make up the $Br^-(CO_2)_n$ solvation shell. The size of the CO_2 shell determined here is larger than that determined for the $I^-(H_2O)_n$ cluster by Markovich *et al.*[25] Overall, the results imply that the solvent shell size decreases as the binding energy of the solute to an individual solvent molecule increases.

The spectra show that there are significant differences between the X^-/N_2O and X^-/CO_2 clusters. Specifically, the CO_2 solvent molecules in the clusters are distorted from linearity, whereas the N_2O molecules are not. This difference as well as the lower SSE's for the X^-/N_2O clusters are attributed to the slightly smaller quadrupole moment in N_2O relative to CO_2.

The vibrational features in the $X^-(CO_2)_n$ data, which are assigned to excitation of an in-phase CO_2 bending vibration upon photodetachment of the anion cluster, are interpreted in terms of a CO_2 distortion in the anion clusters. In the $I^-(CO_2)_n$ clusters, $n=1-4$, simulations indicate that the OCO bond angle is independent of n. This is consistent with pure electrostatic interactions as the cause of the CO_2 distor-

tion. In contrast, simulations of $Br^-(CO_2)_n$ clusters indicate that the CO_2 molecules become slightly more linear as n increases. This may indicate that charge transfer contributes to the solvent/chromophore interaction in the Br^-/CO_2 clusters. In both the $^2P_{1/2}$ band of the $Br^-(CO_2)_n$ spectra and the $^2P_{3/2}$ band of the $I^-(CO_2)_n$ spectra, the vibrational structure becomes unresolved over an intermediate size range and then reappears for the largest clusters. For the $Br^-(CO_2)_n$ spectra, this effect is attributed to greater spectral congestion of the low frequency van der Waals clusters in the intermediate size regime, possibly due to temperature effects. For the $I^-(CO_2)_n$ spectra, the reappearance of structure is attributed to the environment of the $^2P_{3/2}$ I atom becoming more isotropic in the larger clusters.

Overall, the results suggest that the small differences in the composition of the clusters can results on significantly different clustering geometries and dynamics which will conceivably be carried over into the bulk solvation properties. By studying the evolution of the clustering properties as a function of size, it is possible to investigate the interactions which dominate the solvation of negative ions.

ACKNOWLEDGMENTS

This work has been supported by the United States Air Force Office of Scientific Research under Contract No. F49620-94-1-0115. The authors thank Professor Kit Bowen for useful discussions.

[1] Several reviews of ion cluster studies are available; E. J. Bieske and J. P. Maier, Chem. Rev. **93**, 2603 (1993); A. W. Castleman, Jr. and R. G. Keesee, *ibid*. **86**, 589 (1986); R. G. Keesee and A. W. Castleman, Jr., J. Phys. Chem. Ref. Data **15**, 1011 (1986); P. Kebarle, Annu. Rev. Phys. Chem. **28**, 445 (1977).
[2] W. R. Davidson and P. J. Kebarle, J. Am. Chem. Soc. **98**, 6125 (1976).
[3] A. W. Castleman, Jr., P. M. Holland, D. M. Lindsay, and K. I. Peterson, J. Am. Chem. Soc. **100**, 6039 (1978).
[4] K. Hiraoka, S. Mizuse, and S. Yamabe, J. Chem. Phys. **87**, 3647 (1987); K. Hiraoka, Chem. Phys. **125**, 439 (1988).
[5] M. Meot-ner, J. Am. Chem. Soc. **106**, 1265 (1984); M. Samy El-Shall, C. Marks, L. Wayne Sieck, and M. Meotner, J. Phys. Chem. **96**, 2045 (1992).
[6] M. Okamura, L. I. Yeh, and Y. T. Lee, J. Chem. Phys. **88**, 79 (1988); J. M. Price, M. W. Crofton, and Y. T. Lee, *ibid*. **91**, 2749 (1989).
[7] J. A. Draves, Z. Luthey-Schulten, W. L. Liu, and J. M. Lisy, J. Chem. Phys. **93**, 4589 (1990).
[8] C. A. Woodward, J. F. Winkel, A. B. Jones, and A. J. Stace, Chem. Phys. Lett. **206**, 49 (1993).
[9] J.-H. Choi, K. T. Kuwata, B.-M. Haas, Y. Cao, M. S. Johnson, and M. Okamura, J. Chem. Phys. **100**, 7153 (1994).
[10] C. Y. Kung and T. A. Miller, J. Chem. Phys. **92**, 3297 (1990).
[11] E. J. Bieske, A. M. Soliva, A. Friedmann, and J. P. Maier, J. Chem. Phys. **100**, 4156 (1994).
[12] N. E. Levinger, D. Ray, M. L. Alexander, and W. C. Lineberger, J. Chem. Phys. **89**, 5654 (1988).
[13] M. L. Alexander, N. E. Levinger, M. A. Johnson, D. Ray, and W. C. Lineberger, J. Chem. Phys. **88**, 6200 (1988); J. M. Papanikolas, J. R. Gord, N. E. Levinger, D. Ray, V. Vorsa, and W. C. Lineberger, J. Phys. Chem. **95**, 8028 (1991).
[14] T. N. Kitsopoulos, C. J. Chick, A. Weaver, and D. M. Neumark, J. Chem. Phys. **93**, 6108 (1990); D. W. Arnold, S. E. Bradforth, T. N. Kitsolopoulos, and D. M. Neumark, *ibid*. **95**, 8753 (1991); C. C. Arnold, Y. Zhao, T. N. Kitsopoulos, and D. M. Neumark, *ibid*. **97**, 6121 (1992); C. C. Arnold, T. N. Kitsopoulos, and D. M. Neumark, *ibid*. **99**, 766 (1993); C. C. Arnold and D. M. Neumark, *ibid*. **99**, 3353 (1993); **100**, 1797 (1994).
[15] O. Cheshnovsky, S. H. Yang, C. L. Pettiette, M. J. Craycraft, Y. Liu, and R. E. Smalley, Chem. Phys. Lett. **138**, 119 (1987); S. H. Yang, K. J. Taylor, M. J. Craycraft, J. Conceicao, C. L. Pettiette, O. Cheshnovsky, and R. E. Smalley, *ibid*. **144**, 431 (1988); K. J. Taylor, C. L. Pettiette-Hall, O. Cheshnovsky, and R. E. Smalley, J. Chem. Phys. **96**, 3319 (1992).
[16] D. G. Leopold, J. Ho, and W. C. Lineberger, J. Chem. Phys. **86**, 1715 (1987); J. Ho, K. M. Ervin, and W. C. Lineberger, *ibid*. **93**, 6987 (1990).
[17] G. Ganteför, M. Gausa, K. H. Meiwes-Broer, and H. O. Lutz, Faraday Discuss. Chem. Soc. **86**, 197 (1988); J. Chem. Soc. Faraday Trans. 2 **6**, 2483 (1990).
[18] K. M. McHugh, J. G. Eaton, G. H. Lee, H. W. Sarkas, L. H. Kidder, J. T. Snodgrass, M. R. Manaa, and K. H. Bowen, J. Chem. Phys. **91**, 3792 (1989); J. V. Coe, G. H. Lee, J. G. Eaton, S. T. Arnold, H. W. Sarkas, K. H. Bowen, C. Ludewigt, H. Haberland, and D. R. Worsnop, *ibid*. **92**, 3980 (1990).
[19] M. J. deLuca, B. Niu, and M. A. Johnson, J. Chem. Phys. **88**, 5857 (1988); M. J. deLuca, C.-C. Han, and M. A. Johnson, *ibid*. **93**, 268 (1990).
[20] C.-Y. Cham, G. Ganteför, and W. Eberhardt, J. Chem. Phys. **99**, 6308 (1993); H. Handschuh, G. Ganteför, P. S. Bechthold, and W. Eberhardt, *ibid*. **100**, 7093 (1994).
[21] J. V. Coe, J. T. Snodgrass, C. B. Friedhoff, M. K. McHugh, and K. H. Bowen, J. Chem. Phys. **83**, 3169 (1985); **87**, 4302 (1987); J. G. Eaton, S. T. Arnold, and K. H. Bowen, Int. J. Mass Spectrom. Ion Proc. **102**, 303 (1990); G. H. Lee, S. T. Arnold, J. G. Eaton, H. W. Sarkas, K. H. Bowen, C. Ludewigt, and H. Haberland, Z. Phys. D **20**, 9 (1991).
[22] D. W. Arnold, S. E. Bradforth, E. H. Kim, and D. M. Neumark, J. Chem. Phys. **97**, 9468 (1992).
[23] D. M. Cyr, G. A. Bishea, M. G. Scarton, and M. A. Johnson, J. Chem. Phys. **97**, 5911 (1992); D. M. Cyr, M. G. Scarton, and M. A. Johnson, *ibid*. **99**, 4869 (1993).
[24] G. Markovich, R. Giniger, M. Levin, and O. Cheshnovsky, Z. Phys. D **20**, 69 (1991).
[25] G. Markovich, R. Giniger, M. Levin, and O. Cheshnovsky, J. Chem. Phys. **95**, 9416 (1991); G. Markovich, S. Pollack, R. Giniger, and O. Cheshnovsky, Z. Phys. D **26**, 98 (1993).
[26] A. Nakajima, T. Taguwa, and K. Kaya, Chem. Phys. Lett. **221**, 436 (1994).
[27] D. W. Arnold, S. E. Bradforth, E. H. Kim, and D. M. Neumark, J. Chem. Phys. **102**, 3493 (1995).
[28] Y. Zhao, C. C. Arnold, and D. M. Neumark, J. Chem. Soc. Faraday Trans. 2 **89**, 1449 (1993).
[29] R. B. Metz, A. Weaver, S. E. Bradforth, T. N. Kitsopoulos, and D. M. Neumark, J. Phys. Chem. **94**, 1377 (1990).
[30] M. A. Johnson, M. L. Alexander, and W. C. Lineberger, Chem. Phys. Lett. **112**, 285 (1984).
[31] W. C. Wiley and I. H. McLaren, Rev. Sci. Instrum. **26**, 1150 (1955).
[32] J. R. Yamdagni and P. Kebarle, J. Am. Chem. Soc. **94**, 2940 (1972).
[33] L. Perera and M. L. Berkowitz, J. Chem. Phys. **99**, 4222 (1993); L. S. Sremaniak, L. Perera, and M. L. Berkowitz, Chem. Phys. Lett. **218**, 377 (1994); L. Perera and M. L. Berkowitz, J. Chem. Phys. **100**, 3085 (1994).
[34] L. X. Dang and B. C. Garrett, J. Chem. Phys. **99**, 2972 (1993).
[35] J. E. Combariza, N. R. Kestner, and J. Jortner, J. Chem. Phys. **100**, 2851 (1994).
[36] M. A. Walsh, T. H. England, T. R. Dyke, and B. J. Howard, Chem. Phys. Lett. **142**, 265 (1987).
[37] L. Parera and F. G. Amar, J. Chem. Phys. **90**, 7354 (1989); F. G. Amar and L. Perera, Z. Phys. D **20**, 173 (1991).
[38] S. T. Arnold, J. H. Hendricks, and K. H. Bowen, J. Chem. Phys. (in press).
[39] M. R. Battaglia, A. D. Buckingham, D. Neumark, R. K. Pierens, and J. H. Williams, Mol. Phys. **43**, 1015 (1981).
[40] L. H. Sharpen, J. S. Muenter, and V. W. Laurie, J. Chem. Phys. **53**, 2513 (1970).
[41] A. D. Buckingham, C. Graham, and J. H. Williams, Mol. Phys. **49**, 703 (1983).
[42] E. B. Wilson, Jr., J. C. Decius, and P. C. Cross, *Molecular Vibrations* (Dover, New York, 1980), pp. 27–31. The case for two harmonic oscillators is illustrated. We assume this describes the CO_2 bending motion for the $n=2$ cluster. The $2^{1/2}$ term (and, more generally, the $n^{1/2}$ term) results from normal coordinate normalization.
[43] H. S. W. Massey, *Negative Ions* (Cambridge University, Cambridge, 1976); K. Ervin, J. Ho, and W. C. Lineberger, J. Chem. Phys. **91**, 5974 (1991).
[44] C. E. Klots, J. Phys. Chem. **92**, 5864 (1988).
[45] W. G. Lawrence and V. A. Apkarian, J. Chem. Phys. **101**, 1820 (1994).